Transport and Communications Science Journal

MULTI-FREQUENCY SEA LEVEL VARIATIONS AT THE QUY NHON PORT AREA IN THE PERIOD FROM 1987-2023

Pham Minh Trang[1*], Vu Duy Vinh[2], Alexis Chaigneau[3,4]

[1]University of Transport and Communications, No 3 Cau Giay Street, Hanoi, Vietnam

[2]Institute of Science and Technology for Energy and Environment (ISTEE), 246 Danang Street, Haiphong, Vietnam

[3]Université de Toulouse, LEGOS (CNES/CNRS/IRD/UT3), Toulouse, France

[4]Department of Water – Environment – Oceanography, University of Science and Technology of Hanoi (USTH), Vietnam Academy of Science and Technology (VAST), Hanoi, Vietnam

ARTICLE INFO

TYPE: Research Article
Received: 21/03/2025
Revised: 06/05/2025
Accepted: 09/05/2025
Published online: 15/05/2025
https://doi.org/10.47869/tcsj.76.4.13

* Corresponding author
Email: pmtrang@utc.edu.vn; Tel: +84358890279

Abstract. The Quy Nhon port in Vietnam is a key hub for trade and economic development in Binh Dinh province but is significantly impacted by sea-level (SL) variability, which can affect shipping and port operations. This study analyzes sea level variations at Quy Nhon port from 1987 to 2023 using monthly tide gauge data. The Empirical Mode Decomposition method applied to this dataset, identifies four dominant modes: an annual cycle (53.7% of variance, 23.7 cm amplitude) primarily driven by monsoon wind reversals, a semi-annual cycle (27.1%, 13.2 cm amplitude), and interannual (2.3 years, 7 cm amplitude) and decadal (10.7 years, 4 cm amplitude) variations. These latter modes are significantly anti-correlated with the El Niño-Southern Oscillation (ENSO, r = -0.34) and Pacific Decadal Oscillation (PDO, r = -0.45), indicating that warm (cold) phases of these climate modes correspond to lower (upper) SL. A long-term linear SL rise of 1.5 ‑ 2.1 mm/yr was also observed. These findings provide key insights for SL forecasting and maritime safety, emphasizing the need to refine predictions and better understand underlying physical processes.

Keywords: sea-level variability, seasonal and interannual variations, ENSO, PDO, EMD, Quy Nhon port.

1. INTRODUCTION

Ports are the primary interface between sea and land transport networks, playing an important role in international trade with more than 90% of the world's freight [1]. Since ports are located on coastlines or in estuaries, the effectiveness of port operations is directly impacted by sea-level (SL) variation. Extreme SL rises can lead to flooding, inundation and coastal erosion, reducing freeboard in berthing areas and affecting the stability of port structure [2]. Conversely, significant SL drops can cause vessels to run aground when entering and leaving ports, causing significant disruptions to waterway traffic and port operations [1]. Therefore, documenting and understanding SL variations is of primary importance for safe and efficient port operations, including the management of navigational channel depths, planning of maritime traffic, and the protection of coastal infrastructures [3].

Coastal SL variations are influenced by various interacting factors such as tides [4-5], wind [6-8], atmospheric pressure [9-10], rainfall and river discharge [11] as well as steric expansion due to temperature and salinity changes [10,12-13]. These drivers cause SL fluctuations across a wide range of time scales, from short-term tidal cycles [4,14], to long-term climate-induced changes [3,15,17-19]. SL variability has many great impacts on the coastal areas, such as submergence, flooding, saltwater intrusion and coastal erosion, thereby affecting the stability and operation of seaport facilities located on the coast. Therefore, sea level is one of the main characteristics for planning, designing and operating sea port facilities. In the TCVN 21180-2017 standard, the design water level of marine structures is determined based on seasonal, annual and decadal data series [20]. In accordance with the depth specification notice of Ministry of Transport, the minimum depth of water in Quy Nhon port relative to chart datum is announced annually, e.g. 7.4 m in 2018 [21]. Therefore, various studies on SL variability have been conducted in Vietnam and in the world**.** On shorter time scales along the Vietnamese East Sea coasts, semi-diurnal and diurnal SL fluctuations are primarily driven by tides, while seasonal SL changes are influenced by monsoon-driven wind reversals, associated variations in oceanic currents [6-8,22-24]. At interannual and decadal time scales, SL fluctuations are commonly observed [3,15-19].

Several recent studies show that climate change and the El Niño-Southern Oscillation (ENSO) are major factors influencing SL variations [18,25-26]. ENSO, which results from ocean-atmosphere interactions, plays a key role in SL variability, redistributing seawater at both local and regional scales [25,27]. Across the Pacific Ocean, SL changes are closely linked to ENSO, with its effects becoming more pronounced as global warming intensifies [18, 25-26]. In the East Sea off Vietnam, ENSO influences SL through mechanisms such as anomalous water transport or sea surface temperature variations [17,28-29]. At even longer timescales, climate change is driving a sustained global sea-level rise (SLR), with increasingly severe consequences for coastal regions. The Intergovernmental Panel on Climate Change (IPCC) has reported an accelerating global SLR trend, increasing from 1.3 mm/yr (1900-1970), to 1.9 mm/yr (1971-2006) and 3.7 mm/yr (2006-2018) [30]. According to the Ministry of Natural Resource and Environment 2016 (MONRE) reported that Satellite altimetry suggests a regional SLR rate of **3**.3 mm/yr (1993–2014) [31]. The MONRE 2021 reported that SL in Binh Dinh rose with the rate of 5.6mm/yr in recent years and increased 32 cm by 2050, compared to the end of the 20th century, which would threaten the coastal structures like Quy Nhon port [32-33]. Additionally, using the altimetry data from X-TRACK/ALES product, the trends and variability of sea level in 4 tide gauge sites were investigated. The study indicated that the rate of SLR in Quy Nhon (4.96 ÷1.96 mm/year) is

lower than Hon Dau (7.3÷1.75mm/year) but higher than other regions of Vietnam such as Son Tra (0.42÷3.5 mm/year) and Vung Tau (1.11÷4.66 mm/year) [34]. Despite various studies on the long-term rising trend of SL in Vietnam, SL variations at monthly, seasonal and interannual scales in port areas remain insufficiently addressed. In addition, limited studies are available that quantify the ENSO impact on SL variability. The studies [35-36] applied the Empirical Mode Decomposition (EMD) method to evaluate SL trend and variations in different time scales and the impact of ENSO on SL changes at Hon Dau station from 1960-2020. The studies indicated that the rate of annual SLR was 3.56 mm/yr (1960-2020) and 7.78 mm/yr (2002-2020) and the ENSO in the 2÷6.1 year cycle has a great contribution on SL fluctuation in the Hai Phong coastal area with the Intrinsic Mode Function (IMF) 4.5.

Similarly, the Pacific Decadal Oscillation (PDO), a longer-term climate variability mode, can also affect SL in the region. The PDO modulates oceanic and atmospheric conditions over the North Pacific on decadal time scales, influencing sea surface temperature patterns, wind stress, and ocean circulation [37-38]. In Vietnam, PDO-related SL variations could be linked to changes in monsoon characteristics and intensity, coastal upwelling, and large-scale ocean currents, thereby contributing to long-term fluctuations in coastal sea level. However, the specific impacts of PDO on SL dynamics in Vietnamese waters remain less documented and require further investigation.

A comprehensive understanding of these fluctuations and their forcing mechanisms is essential for improving port management and adaptation strategies. Therefore, this study aims to (1) analyse SL variations on various time scales and the climate change-induced- SLR trend from the Quy Nhon tide gauge record in the period of 1987-2023; (2) quantify the contributions of ENSO and PDO on multi-frequency SL fluctuations based on the EMD method, providing key insights into variations of SL in the Quy Nhon port area.

2. MATERIAL AND METHODS

2.1. The Quy Nhon port area

Quy Nhon Port, located to the east of Quy Nhon city in Binh Dinh province (Figure 1), serves as a national general port and a regional hub within the South-Central Coast seaport group. Situated in Quy Nhon Bay and sheltered by Phuong Mai peninsula, the port is well-protected from winds, making it an ideal location for ships to anchor and for loading and unloading goods all year-round. It can accommodate vessels weighing up to 30,000 DWT. With a strategic location as the gateway to the East Sea of the Central region, the Central Highlands of Vietnam and the Mekong Delta countries, Quy Nhon Port has become a key port in trade activities between Vietnam and regional countries. In 2024, the port was expected to handle 11.6 million tons of goods, making it the third largest in the South-Central Coast region, after Da Nang and Dung Quat Ports. Therefore, Quy Nhon Port has a crucial role in promoting trade and economic development of Binh Dinh province and the wider Central region of Vietnam.

The climate in Quy Nhon port is characterized by a typical tropical monsoon climate, with hot and humid conditions throughout the year. The climate is divided into two distinct seasons: a prolonged dry season from January to August with predominant northeast winds, and a shorter rainy season from September to December, influenced by southwest wind. The annual average rainfall in Binh Dinh province ranges from 1,800 to 3,000 mm, with 65-80% of this rainfall occurring during the rainy season [39]. This intense and concentrated rainfall

often results in severe flooding, further exacerbated by typhoons occurring from September to January.

Quy Nhon port is located at the entrance of the Thi Nai Lagoon (Figure 1), the second largest in Vietnam, receiving large freshwater inflows from the Kon and Ha Thanh rivers, with the average annual discharge of ~60 m^3/s and 15 m^3/s [40], respectively. The flow discharge varies significantly between the two seasons: the flow in November is the largest, accounting for over 30% of the average annual flow, the flow in April is the lowest, accounting for only 0.5-2.5% of the average annual flow [41]. The tidal regime at Quy Nhon port is microtidal, with SL fluctuations ranging from 0.4 m during neap tides to 2.1 m during spring tides, averaging 1.25 m [42].

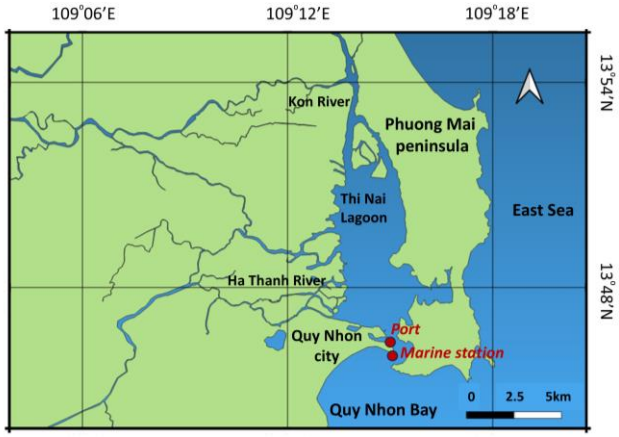

Figure 1. Location of Quy Nhon Port and Quy Nhon Marine station, where sea-level data used in this study were acquired.

2.2. Sea-level data and Empirical Mode Decomposition (EMD) methods

This study used monthly tide gauge records from the Vietnam Hydro-Meteorological Data and Information Center at Quy Nhon Marine Station (13°46'N, 109°15'E) located at the entrance of the port area (Figure 1). The dataset spans 37 years, from January 1987 to December 2023, with SL variations (or anomalies) referenced to the mean SL recorded over this period.

To determine the main mode of SL variability, we applied the Empirical Mode Decomposition (EMD), developed by Huang et al. (1998) [43]. EMD is a commonly used technique for analyzing nonlinear and non-stationary time series. This method decomposes a time series into a set of oscillatory modes, known as intrinsic mode functions (IMFs), and a residual component. The key idea behind EMD, is that any complex signal can be represented as a combination of simpler oscillatory components, each with distinct frequencies, which capture different intrinsic oscillations in the data.

The EMD process is carried out iteratively and involves the following steps:

1. Identifying local extrema: First, the local maxima and minima of the signal are identified.
2. Envelope construction: Upper and lower envelopes are created by connecting the local maxima and minima.
3. Mean subtraction: The mean of these two envelopes is calculated, and the local mean is subtracted from the original signal.

4. Iteration: The result of the subtraction gives a component (often an IMF). If the component does not satisfy IMF criteria, the process is repeated on the residual until a valid IMF is obtained.
5. IMF criteria: Each IMF must satisfy two main conditions:
    - The number of zero-crossings and extrema (local maxima/minima) must be equal.
    - The mean of the upper and lower envelopes at each point must be zero.
6. Residual component: After all IMFs are extracted, the remaining signal is considered the residual, typically corresponding to a long-term trend.

Through this iterative process, different IMFs corresponding to various timescales and frequencies are extracted from the original signal. Each IMF captures a specific mode of variation (e.g., high-frequency fluctuations or long-term trends). In sea-level analysis, this decomposition allows for a better understanding of the processes driving sea-level changes at different temporal scales.

The detailed procedure for EMD can be expressed as:

$$SL(t) = \sum_{j=1}^{M} d_j(t) + r(t) \tag{1}$$

where $SL(t)$ is the original SL timeseries; $d_j(t)$ is the amplitude-frequency modulated oscillatory components (IMFs); and r(t) is the residual term. M is the total number of modes.

According to [44], the average period P_j of each IMF can be calculated based on the length of the original data (n) and the number of peaks of the IMF as follows:

$$P_j = \frac{n}{n_{pj}} \tag{2}$$

where P_j is the mean period of the j^{th} IMF, n is the number of data points in the original time series, and n_{pj} is the number of local peak values in the j^{th} IMF.

To assess the contribution of each IMF mode to the overall signal, the explained variance (EV) of the j^{th} IMF is calculated as:

$$EV_j = \frac{\mathrm{Var}(d_j)}{\mathrm{Var}(SL)} \tag{3}$$

where EV_j is the explained variance of the j^{th} IMF, $Var(d_j)$ is the variance of the j^{th} IMF and $Var(SL)$ is the variance of the original SL timeseries. Since IMFs are not necessarily orthogonal, their explained variances can sum to more than the total variance of the original signal. To account for this, each explained variance is normalized by the total sum of variances, which is 109.9% in our case. Only IMFs that capture a significant portion of the explained variances are retained for further analysis [45].

2.3. Climate indices

To explore the relationship between observed SL variations and large-scale climate patterns, we analyzed two key climate indices: the Oceanic Niño Index (ONI) and the Pacific Decadal Oscillation (PDO). Both indices are important for understanding climate variability, especially in terms of ocean-atmosphere interactions and their influence on global weather systems.

The **ONI** measures sea surface temperature (SST) anomalies in the central and eastern tropical Pacific, particularly in the Niño 3.4 region (from 5°N to 5°S and 120°W to 170°W). It

is widely used to monitor interannual El Niño and La Niña events, which represent the warm and cold phases of the ENSO, respectively. These events significantly affect global weather and oceanic patterns, including those along the Vietnamese coast [35,46-47]. The ONI is calculated as a 3-month running average of SST anomalies in the Niño 3.4 region, with values above +0.5°C for at least 5 consecutive months indicating El Niño conditions and below -0.5°C indicating La Niña [48]. Data were extracted from the NOAA Center for Weather and Cimate Prediction data (http://www.cpc.ncep.noaa.gov).

The **PDO** is a long-term ocean-atmosphere pattern that reflects SST anomalies in the North Pacific Ocean on decadal timescales. It alternates between two phases: the positive phase (characterized by warmer SSTs in the central and northern Pacific) and the negative phase (marked by cooler SSTs). The PDO influences weather and climate patterns across the Pacific, including Southeast Asia [48]. It is monitored through SST anomalies in the North Pacific, specifically between 20°N and 60°N. Data are available from the NOAA.

3. RESULT AND DICUSSION

3.1. General sea level variations and empirical mode decomposition

Figure 2 shows the original monthly SL variations at the Quy Nhon Marine Station from 1987 to 2023. The dataset exhibits strong seasonal variation, with a typical range of ±30 cm. The highest amplitude was 37.6 cm in October 2020, while the lowest was and -28.2 cm in June 1993. From 2007 onwards, larger amplitude values became more frequent, with many occurrences exceeding 30 cm.

In addition to these prominent apparent seasonal oscillations, other higher or lower frequency variations can also be observed. To better identify the main modes of sea-level variability, we applied the EMD method. The four dominant mode functions (IMFs), accounted for 27.1%, 53.7%, 4.4% and 12.3% of the total variance, respectively. Together, these IMFs explain 97.5% of the total variance and correspond to different timescales: the semi-annual cycle (IMF1, 27.1%), the annual cycle (IMF2, 53.7%), the interannual cycle (IMF3, 4.4%), and the decadal cycle (IMF4, 12.3%) with average periods of 0.5 years, 1.0 year, 2.3 years and 10.7 years, respectively. We now describe each of these modes, from seasonal to interdecadal timescales, along with the long-term SL trend.

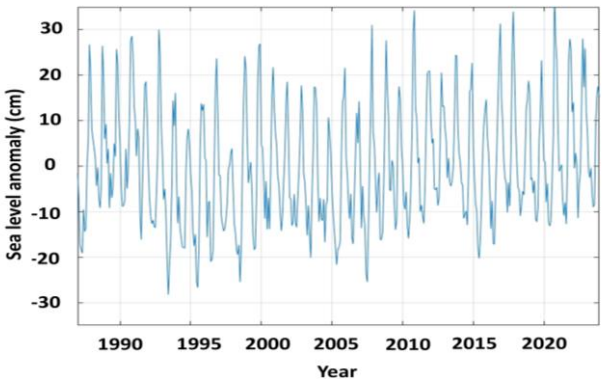

Figure 2. Monthly sea-level anomalies from 1987 to 2003

3.2. Annual and semi-annual sea-level variations

Figure 3 shows the SL variations corresponding to the dominant annual IMF2. The annual SL amplitude mostly varies within a range of ±15 cm, but reaching a maximum of

21.7 cm in December 1992, and a minimum of -21.5 cm in June 1993. A disruption in the annual cycle was observed during 1996-1997 and 2000-2001.

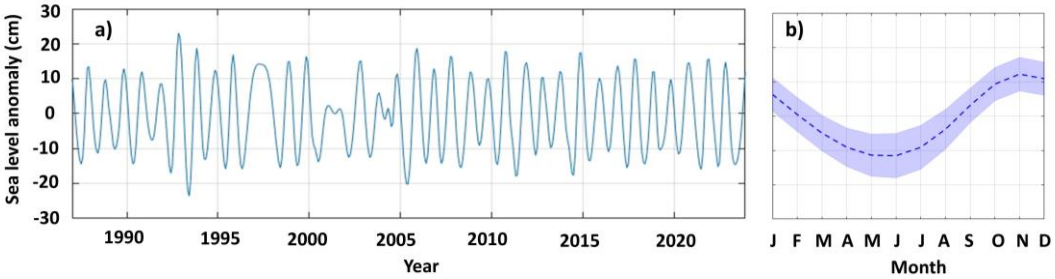

Figure 3. a) The second Intrinsic Mode Function (IMF2), which explains 53.7% of the total variance of the original sea level (SL) data shown in Figure 2. This mode captures the annual variations, with a mean period of 1 year. b) Mean annual cycle (dashed line) and ±1 SD (shaded area) around the mean derived from IMF2.

To better describe the annual SL variation, we computed the mean monthly annual cycle (Figure 3b) from IMF2. The results show two distinct phases. From November to May-June, SL significantly decreases of 23.7 cm, from 12.2 cm in November to -11.5 cm in May-June.

Figure 4 shows the SL variations corresponding to the semi-annual IMF (IMF1), which accounts for 27,1% of the total variance. The semi-annual amplitude generally varies within a range of approximately ± 10 cm, but reached a maximum value of 18.4 cm in October 2020 and a minimum value of -24.1 cm in July 2021. The mean monthly semi-annual cycle derived from IMF1 (Figure 4b) has a maximum amplitude of 13.2 cm, with peak values in May (1.1 cm) and October-November (6.1 cm), while minimum values occur in January-February (-3.5 cm) and August (-7.1 cm).

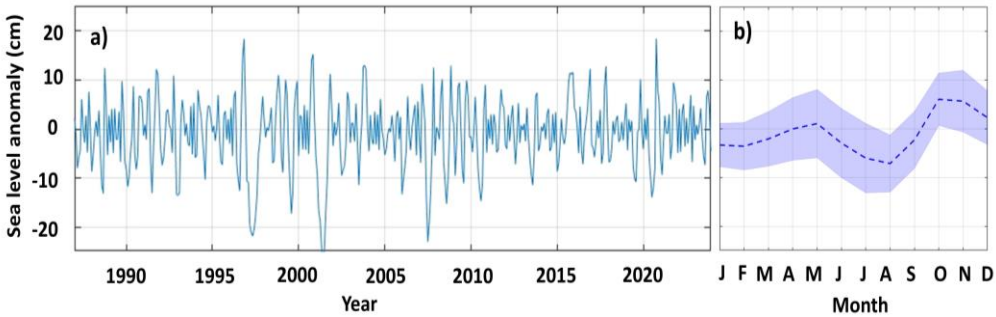

Figure 4. a) The first Intrinsic Mode Function (IMF1), which explains 27.1% of the total variance of the original sea level (SL) data shown in Figure 2. This mode captures the semi-annual variations, with a mean period of 0.5 year. b) Mean semi-annual cycle (dashed line) and ±1 SD (shaded area) around the mean derived from IMF1.

To summarize these initial findings, Table 1 provides the mean monthly statistics of SL derived, from the original time series, thus incorporating both annual and semi-annual cycles. The monthly SL is primarily driven by the annual-cycle, with the lowest mean SL values, around -13 cm, occurring in June-July. From July onward, the average monthly SL steadily increases, reaching a peak of +19.8 cm in November, before decreasing again from November to July. The standard deviation of the monthly mean SL varies between 4.9 cm in September and 7.9 cm in October-November. These results are in agreement with previous studies of seasonal SL variations at the regional scale [10,47].

Table 1. Statistical summary of monthly sea-level anomalies (cm) at the Quy Nhon Marine Station (1987-2023). SD denotes Standard Deviation.

Month	Maximum	Minimum	Mean	SD (cm)
January	16.0	-6.8	4.3	6.0
February	14.1	-13.6	-1.7	6. 8
March	6.1	-17.3	-5.5	6.0
April	8.2	-18.5	-7.5	6.7
May	6.3	-21.6	-8.7	6.6
Jun	3.8	-28.2	-12.8	6.5
July	-3.3	-26.7	-13.4	6.3
August	5.0	-18.6	-9.1	5.8
September	13.7	-7.5	2.6	4.9
October	37.6	0.2	17.2	7.9
November	34.3	2.7	19.8	7.9
December	31.3	2.9	15.1	7.4
Average	14.4	-12.8	0.0	6.55

3.3. Interannual sea-level variations

Figure 5 shows the SL variations corresponding to the interannual IMF3, explaining 4.4% of the total variance. The interannual amplitude typically varies between ±5 cm, reaching the highest value (5.8 cm) in July 2001 and the lowest value (-6.0 cm) in December 2015. As shown in Figure 5, the interannual SL variations are significantly anti correlated with the ONI ($r = -0.34$, $p<0.05$), suggesting that warm ENSO phases (El Niño) are generally associated with a decrease in SL, while cold ENSO phases (La Niña) correspond to an increase in SL (Figure 5).

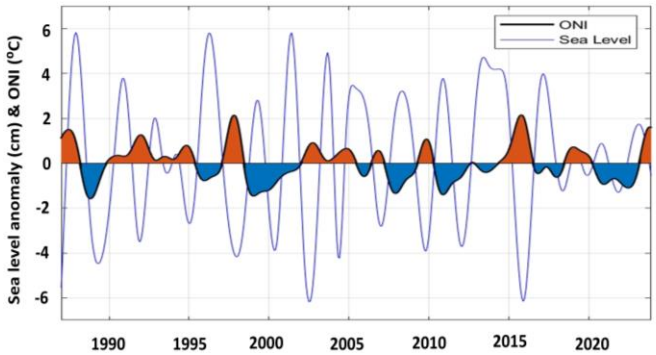

Figure 5. The third Intrinsic Mode Function (IMF3, blue line), which explains 4.4% of the total variance of the original sea level (SL) data shown in Figure 2. This mode captures the interannual variations, with a mean period of 2.3 years. Superimposed on the IMF3 is the Oceanic Niño Index (ONI) (black line), low-pass filtered with a cutoff period of 4 years. El Niño (warm) and La Niña (cold) phases are highlighted with red and blue shaded areas, respectively.

3.4. Interdecadal and long-term sea-level variations

Figure 6 shows the SL variations corresponding to the interdecadal Intrinsic Mode Function (IMF4), which explains 12.3% of the total variance. The interdecadal amplitude typically ranged between ±5 cm, with the highest value recorded at the end of the 1980s (11.3 cm) and the lowest in 1995 (-9.0 cm). The interdecadal SL amplitude has generally shown a decreasing trend since the 1980s. The correlation between interdecadal SL variations and the

Pacific Decadal Oscillation (PDO) is negative (r = -0.45), indicating that a warm PDO phase is associated with a decrease in sea level, while a cold PDO phase corresponds to an increase in SL at Quy Nhon.

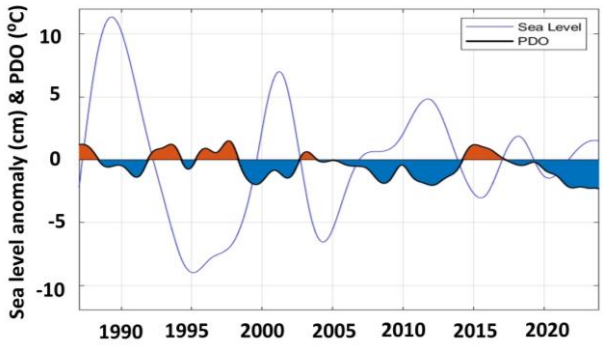

Figure 6. The fourth Intrinsic Mode Function (IMF4, blue line), explaining 12.3% of the total variance of the original sea level (SL) data shown in Figure 2. This mode captures the decadal variations, with a mean period of 10.7 years. Superimposed on the IMF is the Pacific Decadal Oscillation (PDO) data (dark line), low-pass filtered with a cutoff period of 10 years. Positive (warm) and negative (cold) phases are highlighted with red and blue shaded areas, respectively.

The long-term SL trend was assessed using 2 approaches: linear regression on yearly SL time series (Figure 7) and Sen's slope estimator [49-50] with the Mann-Kendall test [51-52]. Results indicate a significant positive trend ($p<0.01$), with SLR estimates ranging from 1.5 mm/yr (linear regression) to 2.1 mm/yr (Sen's slope estimation).

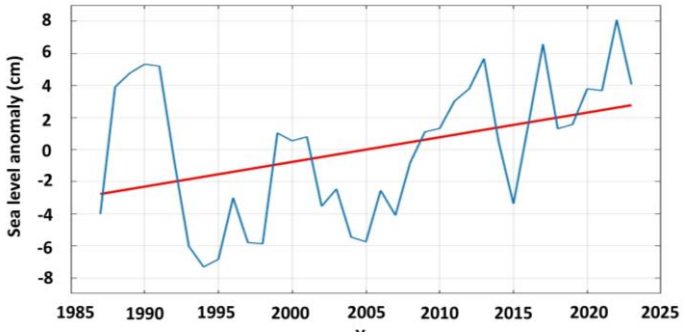

Figure 7. Yearly sea-level variations (blue line) derived from the original sea level data in Figure 2. The linear trend of sea-level rise (red line) indicated an increase of 1.5 mm/yr over the study period (1987-2023).

3.5. Discussion

Seasonal cycle of sea-level variations

The seasonal SL variation observed in this study is consistent with previous findings based on altimetry data and model outputs [47], showing a decrease from December to June and an increase from June to December. However, this slightly differs from results in [10], where SL anomalies increased gradually from December to February, peaking at +10 cm under the influence of northeasterly (NE) winds, followed by a decline from March to May (-5 cm) with southeasterly (SE) winds and from June to August (-10 cm) under southwesterly (SW) winds. A rapid rise (+5 cm) was observed from September to November, making the onset of NE winds.

These seasonal SL variations are primarily driven by the reversing Southeast Asian monsoon. Wind forcing significantly impacts oceanic current and circulation through Ekman

transport and geostrophic adjustment, which in turn affects SL in the Quy Nhon port area. Additionally, the study area also interacts with the Pacific Ocean through the Luzon Strait and is subject to monsoon-driven circulation patterns [47]. In winter, strong NE winds induce cyclonic circulation in the East Sea of Vietnam, driving a southward alongshore current associated with an increase in coastal SL. Conversely, in summer, SW winds induce an anticyclonic gyre in the northern region and a cyclonic gyre in the southern part. This well-documented dipole structure includes an eastward jet that transports water offshore, lowering SL at the coast [53].

Using a simple barotropic model, a recent study demonstrated that wind forcing is the primary driver of SL variability in the region, accounting for 16.9 cm of annual and semi-annual SL variations at Quy Nhon [10]. Other key drivers include steric effects (2.7 cm) and atmospheric pressure via the inverse barometer effects (4.3 cm) [10]. The semi-annual SL cycle also closely follows the semi-annual wind cycle. However, the contributions of steric components (2.9 cm) and wind setup (2.5 cm) further emphasize the role of these forcings in semi-annual SL variation [10]. Additionally, the seasonal changes in precipitation and river runoff as discussed in Section 2.2, can also contribute to the SL coastal variability in semi-annual and annual time scales.

Interannual and decadal variation

The interannual variability in sea level is related to fluctuations in atmospheric pressure and wind patterns, which are, in turn, connected to climate indices like ENSO. Additionally, this variability has been linked to changes in ocean currents in the Northwest Pacific, as well as variations in steric height and sea surface temperature.

Our results suggested a link between SL variability and ENSO events. Maximum negative SL anomalies were detected during canonical El Nino periods (1998, 2007 and 2015) or El Nino Modoki periods (2004 - 2005), whereas maximum positive SL anomalies occurred in the transition from La Nina Modoki to neutral (2001 and 2013), in the La Nina Modoki period (1999) and in the La Nina period (2017), in agreement with [46]. El Niño Modoki refers to a distinct type of El Niño characterized by warmer sea surface temperatures (SSTs) in the central Pacific, flanked by cooler SSTs in the eastern and western Pacific. Unlike conventional or canonical El Niño events, which strongly influence the western Pacific through large-scale oceanic and atmospheric anomalies, El Niño Modoki has a more complex impact on regional SL variations due to its different wind and thermocline response patterns. This distinction highlights the nuanced influence of ENSO on coastal SL variations in Quy Nhon.

The anti-correlation between sea level and ENSO observed in this study is consistent with previous findings [17-18,54] and results from coupled ocean-atmosphere processes. During the development of El Niño, an increased inflow of cold water through the Luzon Strait causes an anomalous cooling, contributing to a sea level drop in the South China Sea (SCS) through the thermosteric effect [54]. At the same time, an abnormally weak high-pressure cell establishes over the western Pacific [55], altering wind patterns and generating an anomalous cyclonic circulation in the SCS. This circulation leads to surface water divergence and an uplift of the thermocline due to Ekman pumping, further lowering sea level. Finally, an anomalous atmospheric subsidence over the SCS [56-57] reduces convection and precipitation during El Niño years [46,58]. This decline in precipitation significantly contributes to the persistence of negative sea level anomalies, leading to a drop of a few cm

[54]. Conversely, these processes reverse during La Niña, promoting sea level rise in the SCS and along the Vietnamese coasts.

Furthermore, as mentioned above, monsoon wind forcing is a dominant driver of SL variation in the Quy Nhon port area. Study [58] showed that during El Niño, elevated atmospheric pressure in Central Vietnam during autumn (September –November) creates northward wind anomalies at the coast. These anomalies can lead to an increase offshore Ekman Transport and explain the SL reduction observed at the coast during El Niño events. Conversely, lower atmospheric pressure anomalies during La Niña generate southward wind anomalies, that could enhance onshore Ekman transport and increase SL at the coast.

In addition, rainfall and river discharge may slightly contribute to SL changes during ENSO events. Study [58] found that annual rainfall in Central Vietnam increased by over 10% during La Niña years but decreased by around 30% during El Niño. Specifically, at Quy Nhon, autumn rainfall rose by 20 mm during La Niña periods and decreased by up to 60 mm during El Niño. Herrmann et al. (2023) further noted a reduction in summer rainfall (June-August) during El Niño and El Niño Modoki, while winter rainfall (December- February) increased during La Niña and La Niña Modoki [46]. The proximity of the Quy Nhon marine station to the Kon and Ha Thanh river mouths and the Thi Nai lagoon (Figure 1) may amplify its SL variations' sensitivity to river flow fluctuations driven by rainfall changes during ENSO events. This influence may further reinforce the anti-correlation observed between SL and the ONI index.

It is important to note that the interannual IMF3, which we primarily associated with ENSO, has a mean time period of 2.3 years. This duration also corresponds to the atmospheric Quasi-Biennial Oscillation (QBO), a periodic shift in the dominant direction (either easterly or westerly) of equatorial stratospheric winds [59]. These alternating wind patterns gradually descend and dissipate near the tropopause [60]. Although some studies have reported significant relationships between the QBO index and sea level in the tropical South Atlantic [61] or near polar regions [62], the dynamical link between this stratospheric mode and sea level remains largely unexplored. Our results suggest that a similar connection between the QBO and sea level variability may exist along the Vietnamese coast. However, a detailed investigation of this relationship in the Vietnam East Sea is still lacking and require further study.

Regarding decadal SL variations, recent studies in the Pacific, suggested that they are primarily driven by the modulation of the steric component and fluctuations in Pacific trade winds associated with modulation of large-scale climate modes. Additionally, the increasing frequency, intensity, and duration of some extreme weather events (e.g., heat waves, severe storms, droughts, floods) further influence SL variations in the context of ongoing climate changes [37,38].

The study by [37] examined the key drivers of decadal sea level (SL) variability in the Pacific Ocean and found that the PDO influences SL in the Vietnam East Sea through oceanic processes originating in the western tropical Pacific. During the cold PDO phase (1993–2009), intensified trade winds strengthened downwelling Rossby waves and upwelling Kelvin waves, steepening the thermocline across the tropical Pacific and reinforcing the Walker Circulation. This period also saw a strengthening of the North Equatorial, Mindanao, and Kuroshio Currents, while the South China Sea Throughflow weakened. Similarly to what happens during cold ENSO phases, the reduction of the transport through the Luzon Strait may favor warmer water and higher SL along the Vietnamese coast. In contrast, during the

warm PDO phase (2010–2019), the Walker Circulation and major currents weakened, while the South China Sea Throughflow strengthened transporting more colder water along the Vietnamese coast. These large-scale circulation changes resulted in SL rise during the cold PDO phase and SL decline during the warm phase [37], consistent with our findings and the observed anti-correlation between coastal SL in Quy Nhon and the PDO index.

Additionally, the PDO affects atmospheric pressure along the Vietnam coast, decreasing during the cold phase and increasing during the warm phase [38]. This variation amplifies SL fluctuations through the inverse barometer effect, enhancing SL rise during cold PDO phases and contributing to SL decline during warm phases.

Long-term sea-level rise

Based on Sen's approach and a linear regression analysis, the average annual rate of SLR in Quy Nhon ranged from 1.5 mm/yr to 2.1 mm/yr over the period 1987-2023. In comparison, Hai Phong experienced a higher rate of 3.6 mm/yr, which further accelerated to 7.8 mm/yr from 2002 to 2020. Additionally, the rate of SLR in Quy Nhon obtained from Sen's approach was 6.0 mm/yr during 2002-2018 and higher than the result of 5.0 mm/yr in the study [34] using the CEEMDAN method.

SLR is subject to considerable interest in the context of global warming. This rise results from two major processes: the thermal expansion of the ocean due to increasing ocean heat content, and the inflow of freshwater into the ocean caused by the melting of polar ice caps, mountain glaciers, and potential exchanges with continental water reservoirs [63].

4. CONCLUSION

This study investigated temporal SL variations in the Quy Nhon port area using a long-term (1987-2023) and high frequency (monthly) dataset from a coastal tide station. The results highlight significant seasonal (annual and semi-annual), interannual, and decadal SL variations, alongside a long-term rising trend.

Using the EMD method, 4 dominant SL variation modes were identified. The annual cycle (IMF2, 1-year period) explains 53.7% of the total variance, with SL rising from May-June to November and declining from November to May-June, exhibiting an amplitude of 23.7 cm. The semi-annual cycle (IMF1, 0.5-year period) accounts for 27.1% of the variance, with a maximum amplitude of 13.2 cm. This component features two distinct phases: an increase from January-February to May and from August to October-November, followed by a decrease from May to August and from October-November to January-February. While seasonal SL variations are primarily driven by the annual cycle, they are also modulated by the weaker semi-annual component. The main driver of the seasonal variability is likely the monsoon-induced wind reversal and the associated ocean circulation.

The interannual variation (IMF3, 2.3-year period) represents 4.4% of the total variance, while the decadal variation (IMF4, 10.7-year period) accounts for 12.3%. These variations are significantly anticorrelated with ENSO ($r = -0.34$) and PDO ($r = -0.45$), highlighting the influence of large-scale climate modes on SL variability. The higher explained variance of PDO revealed a stronger impact of PDO than ENSO on the Quy Nhon sea level variation. The higher explained variance of the annual and semi-annual cycle show that the local forcings such as monsoon wind, temperature are dominant to remote forcings which are climate patterns (PDO, ENSO,QBO).This is completely consistent with the previous study [34].

A statistically significant long-term increase in sea level was also observed, with rates ranging from 1.5 to 2.1 mm/year during 1987-2023, but reaching to 6 mm/year during 2002-2018 which is lower than in Hai Phong but higher than other coastal areas in Vietnam.

These findings provide valuable benchmarks for SLR prediction and maritime safety in the Quy Nhon port area. As SL variations impact vessel manoeuvrability, port operations, and future adaptation strategies, further research should focus on refining SL forecasts and deepening our understanding of the underlying drivers and physical mechanisms. Such efforts will be important to ensuring safe navigation and efficient port operations in the coming decades.

ACKNOWLEDGMENT

This research is funded by University of Transport and Communications (UTC) under grant number T2025-CT-001.

REFERENCES

[1]. T. H. Chang, H. Y. Wang, Analysis and Exploration of the Impact of Average Sea Level Change on Navigational Safety in Ports, Water, 15 (2023) 2570. https://doi.org/10.3390/w15142570
[2]. V. Gracia, Assessing the impact of sea level rise on port operability using LiDAR-derived digital elevation models, Remote Sens. Environ, 232 (2019) 111318.
[3]. T. M. El-Geziry, Y. M. El-Wakeel, A decadal sea-level variability in Port-Said Harbour (Egypt), Egypt J. Aquat. Res, 1 (2023) 33–39. https://doi.org/10.1016/j.ejar.2022.08.001
[4]. A. Chaigneau, From seasonal flood pulse to seiche: Multi-frequency water-level fluctuations in a large shallow tropical lagoon (Nokoué Lagoon, Benin), Estuar. Coast Shelf Sci., 267 (2022) 107767.
[5]. J. Valle-Rodríguez, A. Trasviña-Castro, Sea level anomaly measurements from satellite coastal altimetry and tide gauges at the entrance of the Gulf of California, Adv. in Space Res, 7 (2020) 1593-1608. https://doi.org/10.1016/j.asr.2020.06.031
[6]. S. Saramul, T. Ezer, Spatial variations of sea level along the coast of Thailand: Impacts of extreme land subsidence, earthquakes and the seasonal monsoon, Glob Planet Change, 122 (2014) 70-81.
[7]. L. Qinyu, J. Yinglai, W. Xiaohua, Y. Haijun, On the Annual Cycle Characteristics of the Sea Surface Height in South China Sea, Adv. in Atmospheric Sci, 18 (2001) 613-622.
[8]. J. Zhou, P. Li, H. Yu, Characteristics and mechanisms of sea surface height in the South China Sea, Glob Planet Change, 88 (2012) 20–31. https://doi.org/10.1016/j.gloplacha.2012.03.001
[9]. T. Wahl, F. M. Calafat, M. E. Luther, Rapid changes in the seasonal sea level cycle along the US Gulf coast from the late 20th century, Geophys Res Lett, 2 (2014) 491–498.
[10]. A. M. Amiruddin, The seasonal cycle and variability of sea level in the South China Sea, J. Geophys. Res. Oceans, 8 (2015) 5490-5513.
[11]. M. N. Tsimplis, P. L. Woodworth, The global distribution of the seasonal sea level cycle calculated from coastal tide gauge data, J. Geophys. Res, C8 (1994) 16031-16039.
[12]. M. Marcos, M. N. Tsimplis, Variations of the seasonal sea level cycle in southern Europe, J. Geophys. Res. Oceans, C12 (2007) C12011. https://doi.org/10.1029/2006JC004049
[13]. X. Cheng, Y. Qi, On steric and mass-induced contributions to the annual sea-level variations in the South China Sea, Glob. Planet Change, 3 (2010) 227-233.
[14]. J. Zandagba, M. Moussa, E. Obada, A. Afouda, Hydrodynamic modeling of Nokoué Lake in Benin, Hydrology, 3 (2016) 3040044. https://doi.org/10.3390/hydrology3040044
[15]. S. Dangendorf, Characteristics of intra-, inter-annual and decadal sea-level variability and the role of meteorological forcing: The long record of Cuxhaven, Ocean Dyn, 63 (2013) 209–224.
[16]. G. Chen, Z. Wang, C. Qian, C. Lv, Y. Han, Seasonal-to-decadal modes of global sea level variability derived from merged altimeter data, Remote Sens. Environ, 11 (2010) 2524-2535.
[17]. G. Han, Low-frequency sea-level variability in the South China Sea and its relationship to ENSO, Theor. Appl. Climatol, 97 (2009) 403. https://doi.org/10.1007/s00704-009-0116-y

[18]. L. Wang, Q. Li, X. Z. Mao, H. Bi, P. Yin, Interannual sea level variability in the Pearl River Estuary and its response to El Niño–Southern Oscillation, Glob. Planet Change, 162 (2018) 163–174.
[19]. L. S. Genes, R. D. Montoya, A. F. Osorio, Costal Sea level variability and extreme events in Moñitos, Cordoba, Colombian Caribbean Sea, Cont. Shelf Res, 228 (2021) 104489.
[20]. TCVN 11820-2017, Marine Port Facilities-Design Requirements, Minstry of Transport
[21]. Marine notice on water depth specifications in front of Quy Nhon port, Ministry of Transport, 2018. [Online]. Available: www.vms-south.vn.
[22]. S. V. Vinogradov, R. M. Ponte, Annual cycle in coastal sea level from tide gauges and altimetry, J. Geophys. Res. Oceans, C4 (2010) C04021. https://doi.org/10.1029/2009JC005767
[23]. B. Hünicke, E. Zorita, Trends in the amplitude of Baltic Sea level annual cycle, Tellus A: Dynamic Meteo. and Ocean, 1 (2008) 154–164. https://doi.org/10.1111/j.1600-0870.2007.00277.x
[24]. R. R. Torres, M. N. Tsimplis, Seasonal Sea level cycle in the Caribbean Sea, J. Geophys. Res. Oceans, C7 (2012) C07011. https://doi.org/10.1029/2012JC008159
[25]. J. H. Moon, Y. T. Song, H. K. Lee, PDO and ENSO modulations intensified decadal sea level variability in the tropical Pacific, J. Geophys. Res. Oceans, 12 (2015) 8229–8237.
[26]. L. S. Genes, R. D. Montoya, A. F. Osorio, Costal Sea level variability and extreme events in Moñitos, Cordoba, Colombian Caribbean Sea, Cont. Shelf Res, 228 (2021) 104489.
[27]. S. Muis, Influence of El Niño-Southern Oscillation on Global Coastal Flooding, Earths Future, 9 (2018) 1311–1322.
[28]. B. Liu, G. Wu, R. Ren, Influences of ENSO on the vertical coupling of atmospheric circulation during the onset of South Asian summer monsoon, Clim. Dyn., 45 (2015) 1859–1875.
[29]. M. Herrmann, T. T. Duy, Mechanisms and intraseasonal variability of the South Vietnam Upwelling, South China Sea: role of circulation, tides and rivers, 4 (2024) 1013–1033.
[30]. P. Zhai, A. Pirani, S.L. Connors, C. Péan, S. Berger, N. Caud, Y. Chen, L. Goldfarb, M.I. Gomis, M. Huang, K. Leitzell, E. Lonnoy, J.B.R. Matthews, T.K. Maycock, T. Waterfield, O. Yelekçi, R. Yu, B. Zhou, Climate Change 2021: The Physical Science Basis. Contribution of Working Group I to the Sixth Assessment Report of the Intergovernmental Panel on Climate Change, Cambridge University Press, IPCC, 2021
[31]. MONRE, Climate change and sea level rise scenarios for Viet Nam, Hanoi, 2016.
[32]. T. T. Van, T. H. Thai, Climate change impacts and adaptation measures for Quy Nhon city, Ear. and Environ. Sci, 2 (2011) 119-127.
[33]. National Climate Assessment Report, Ministry of Natural Resource and Environment, 2021.
[34]. D. T. Pham, Sea-level trends and variability along the coast of Vietnam over 2002–2018: Insights from the X-TRACK/ALES altimetry dataset and coastal tide gauges, Adv. in Space Res, 3 (2024) 1630–1645. https://doi.org/10.1016/j.asr.2023.10.041
[35]. N. M. Hai, S. Ouillon, V. D. Vinh, Sea-level rise in Hai Phong coastal area (Vietnam) and its response to ENSO-evidence from tide gauge measurement of 1960-2020, Vietnam J. of Earth Sci., 44 (2022) 109–126. https://doi.org/10.15625/2615-9783/16961
[36]. H. M. Nguyen, S. Ouillon, V. D. Vu, Sea Level Variation and Trend Analysis by Comparing Mann–Kendall Test and Innovative Trend Analysis in Front of the Red River Delta, Vietnam (1961–2020), Water, 14 (2022) 1709. https://doi.org/10.3390/w14111709
[37]. X. Cheng, Regime Shift of the Sea Level Trend in the South China Sea Modulated by the Tropical Pacific Decadal Variability, Geophys. Res. Lett, 7 (2023) e2022GL102708.
[38]. W. Qin, Y. Cai, L. He, The Relationship between the Typhoons Affecting South China and the Pacific Decadal Oscillation, Atmosphere, 3 (2024) 285. https://doi.org/10.3390/atmos15030285
[39]. N. Q. Binh, V. H. Cong, V. N. Duong, Assessment of sediment transportation to Thi Nai lagoon, Binh Dinh province, J. of Sci. and Tech. of Water Res. and Environ, 65 (2019) 58–66.
[40]. L.X. Sinh, Assessment of pollution load into Thi Nai lagoon, Viet Nam and prediction to Assessment of Pollution Load into Thi Nai Lagoon, Art. in International J. of Sci, 4, (2015) 117-127.
[41]. People's Committee of Binh Dinh Province, Binh Dinh Gazetteer, Nature, Population and Administration. General Publisher, Quy Nhon, 2005.

[42]. T. T. D. Tran, T. T. Tran, Application of PlanetScope-based Depth Invariant Index method in Seagrass Mapping: The study in Thi Nai Lagoon, Binh Dinh Province, Sci. and Tech. Development J, 24 (2021) 2110-2122. https://doi.org/10.32508/stdj.v24i3.2737
[43]. N. E. Huang, Applications of Hilbert–Huang transform to non-stationary financial time series analysis Appl. Stochastic Models Bus and Indus, 19 (2003) 245-268.
[44]. Z. Wu, N. E. Huang, A study of the characteristics of white noise using the empirical mode decomposition method, Proceedings of the Royal Society A: Mathematical, Physical and Engineering Sciences, (2004) 1597–1611.
[45]. C. Franzke, Multi-scale analysis of teleconnection indices: Climate noise and nonlinear trend analysis, Nonlinear Process Geophys, 1 (2009) 65–76. https://doi.org/10.5194/npg-16-65-2009
[46]. H. N. Thanh, N.D. Thanh, M. Herrmann, The distinct impacts of the two types of ENSO on rainfall variability over Southeast Asia, Clim. Dyn, 61 (2023) 2155–2172.
[47]. N. B. Trinh, New insights into the South China Sea throughflow and water budget seasonal cycle: evaluation and analysis of a high-resolution configuration of the ocean model SYMPHONIE version 2.4, Geosci. Model Dev, 4 (2024) 1831–1867. https://doi.org /10.5194/gmd-17-1831-2024
[48]. NOAA, 2020. https://origin.cpc.ncep.noaa.gov/products/analysis_monitoring/ensostuff/ONI_v5.php. Access on December 31, 2020.
[49]. P. K. Sen, Estimates of the Regression Coefficient Based on Kendall's Tau, J. Am. Stat. Assoc, 63 (1968) 1379–1389. https://doi.org/10.1080/01621459.1968.10480934
[50]. H. Theil, A rank-invariant method of linear and polynomial regression analysis, in: B. Raj, J. Koerts (Eds.) Henri Theil's Contri. to Economi and Economet, Advanced Studies in Theoretical and Applied Econometrics Age, Springer, Dordrecht, 1992. https://doi.org/10.1007/978-94-011-2546-8_20 1992
[51]. H. B. Mann, Nonparametric tests against trend, Econometrica Soci, 13 (1945) 245-259.
[52]. H. Abdi, The Kendall Rank Correlation Coefficient, The Concise Encyclopedia of Statistics (1995) 278-281.
[53]. T. T. Duy, The role of wind, mesoscale dynamics, and coastal circulation in the interannual variability of the South Vietnam Upwelling, South China Sea - answers from a high-resolution ocean model, Ocean Science, 4 (2022) 1131–1161. https://doi.org/10.5194/os-18-1131-2022
[54]. Z. Rong, Y. Liu, H. Zong, Y. Cheng, Interannual sea level variability in the South China Sea and its response to ENSO, Glob. Planet Change, 4 (2007) 257–272.
[55]. R. Huang, W. Chen, B. Yang, R. Zhang, Recent advances in studies of the interaction between the East Asian winter and summer monsoons and ENSO cycle, Adv. Atmos. Sci, 21 (2004) 407–424.
[56]. R. H. Weisberg, C. Wang, A western Pacific oscillator paradigm for the El Niño-Southern Oscillation, Geophys. Res. Lett, 7 (1997) 779–782. https://doi.org/10.1029/97GL00689
[57]. C. Wang, R. H. Weisberg, J. I. Virmani, Western Pacific interannual variability associated with the El Niño-Southern Oscillation, J. Geophys. Res. Oceans, C3 (1999) 5131–5149.
[58]. T. V. Vu, Effects of ENSO on autumn rainfall in central Vietnam, Adv. in Meteo, 1, 264373, 2015.
[59]. G. A. Meehl, The South Asian Monsoon and the Tropospheric Biennial Oscillation, J. of Clim, 8 (1997) 1921-1943.
[60]. P. L. Woodworth, Forcing Factors Affecting Sea Level Changes at the Coast, Surv. in Geophys, 40 (2019) 1351–1397.
[61]. J. A. M. Andrew, H. Leach, P. L. Woodworth, The relationships between tropical Atlantic sea level variability and major climate indices, Ocean Dyn, 56 (2006) 452–463.
[62]. A. Hibbert, Quasi-biennial modulation of the Southern Ocean coherent mode, Quarterly J. of the Royal Meteo.l Soci, 648 (2010) 755–768.
[63]. A. Cazenave, B. Meyssignac, M. Ablain, Global sea-level budget 1993-present, Earth Syst. Sci. Data, 3 (2018) 1551–1590.